# Roles of Interlayers in Efficient Organic Photovoltaic Devices[a]

Jong Hyeok Park, Tae-Woo Lee, Byung-Doo Chin, Dong Hwan Wang,
O Ok Park*

This review discusses interfacial layers in organic photovoltaic devices. The first part of the review focuses on the hole extraction layer, which is located between a positive electrode and an organic photoactive material. Strategies to improve hole extraction from the photoactive layer include incorporation of several different types of hole extraction layers, such as conductive polymeric materials, self-assembled molecules and metal oxides, as well as surface treatment of the positive electrodes and the conductive polymeric layers. In the second part, we review recent research on interlayers that are located between a negative electrode and a photoactive layer to efficiently extract electrons from the active layer. These materials include titanium oxides, metal fluorides and other organic layers.
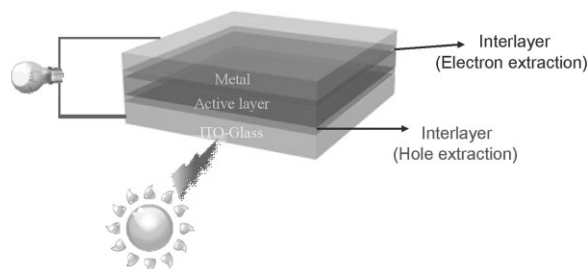
Introduction

Developing high performance organic photovoltaic devices (OPVs) as sources of sustainable energy has been an important issue in research conducted worldwide in recent years due to the low manufacturing cost of the devices and their use in the fabrication of flexible devices. Recent

O. O Park, D. H. Wang
Department of Chemical and Biomolecular Engineering, KAIST, Daejoen 305-701, Korea
E-mail: oopark@kaist.ac.kr
J. H. Park
Department of Chemical Engineering, Sungkyunkwan University, Suwon, Gyeonggi-do, Korea
T.W. Lee
Department of Materials Science and Engineering, Pohang University of Science and Technology, San 31, Hyoja-dong, Nam-gu, Pohang, Gyeongbuk 790-784, Korea
B.D. Chin
Department of Polymer Science and Engineering, Dankook University, Jukjeon, Gyeonggi-do, Korea

[a] J. H. Park and T. W. Lee contributed equally to this work.

outstanding progress in this area has been made mostly by the production of photoactive materials with good morphological control.[1–7] Since the discovery of efficient electron transfer between poly(3-hexyl thiophene) (P3HT) and [6,6]-phenyl C_{61}-butyric acid methyl ester (PCBM), along with the good bulk heterojunction morphology of these compounds in polymer solar cells, considerable attention has been directed toward increasing the power conversion efficiency and long term stability of such systems.[7–15]

Electricity generation from OPVs is accomplished via several steps. Strongly bounded hole and electron pairs, called photo-generated excitons, which are generated by the incident light, split from each other at the interface between the donor and acceptor. The electrons are accepted by materials with a higher electron affinity, and the holes are accepted by materials with a lower ionization potential. Then, the generated electrons and holes are transported through the p-type material and n-type material phases, respectively, toward both electrodes, resulting in an external photocurrent flow. Thus, the overall power conversion efficiency of organic solar cells depends on the combination of the following steps: 1) exciton

generation after absorbing incident solar light; 2) dissociation of the electron-hole pairs at the p-n interface; 3) the transport of electrons and holes to both electrodes; 4) the collection of charges at the electrodes. As a result, the photocurrent does not depend solely on the photogeneration and transport properties of the electrons and holes, but also depends on the interface between the active layer and electrodes. The first three steps are strongly dependent on the nature of the materials used and the morphology of the active materials in the bulk-hetero junction (BHJ). The blend morphology can be controlled by the overall processing conditions, including the dissolving solvent,[16–18] thermal annealing,[9,19,20] solvent annealing [7,21] and incorporation of additives.[14,22–27] Furthermore, efficient organic photovoltaic devices with a donor-acceptor concentration graded photoactive layer prepared through a spin-coating process[28] or a stamping transfer technique[29] have been reported. In particular, devices with concentration graded active layers can be easily fabricated through a spin-coating process by applying a new solvent that can swell just the bottom layer.[30]

The last feature underlying high efficiency OPVs is inserting an interlayer between the active layer and the indium tin oxide (ITO) substrate or the active layer and the metal electrode.[31–37] Considering the recent progress with organic light-emitting diodes (OLEDs), the interlayers in terms of device efficiency and lifetime are extremely important.[38–45] Although interlayers are not active layers involved in the light emission process, they can improve the electroluminescence efficiency several times by several orders of magnitude.[38–45] The same approaches can be applicable to OPVs as well. Until now, state-of-the art OPVs have demonstrated a power conversion efficiency as high as 7.4%.[46] If one can increase the extraction efficiency of holes and electrons generated from the active layer slightly, OPVs may be intensively developed towards commercialization. Even though research on interlayers in OPVs has not yet been fully completed, the number of papers has gradually increased recently. The surface energy of the hole extraction layer on the ITO anode will be important because it can control the chain ordering of the polymeric photoactive layer, which is crucial for charge transport and extraction from the photoactive layer in the devices.[36,47] Therefore, the interfacial layer located between the active layer and the anode in OPVs is important in terms of hole extraction, as well as control of the morphology of the photoactive layer in OPVs. Secondly, interlayers between the active layer and the cathode can serve a number of functions, including protecting active layers from damage during metal evaporation and thereby eliminating exciton quenching at the interface.[48] Moreover, some interlayers at the negative electrode can transfer electrons more efficiently and block the movement of holes from the active layer to the cathode.[49,50]

Jong Hyeok Park is an assistant professor in the School of Chemical Engineering at Sungkyunkwan University (SKKU), Republic of Korea. He received his PhD in chemical engineering from KAIST, Korea, in August 2004. He then joined the University of Texas at Austin, USA, as a postdoctoral researcher in 2004. From March 2007 to February 2008, he worked at the Electronics and Telecommunications Research Institute (ETRI). He is the author and co-author of 94 papers and 33 patents. His research focuses on organic solar cells, dye-sensitized solar cells and solar-to-hydrogen conversion devices.

Tae-Woo Lee is an assistant professor in the Department of Materials Science and Engineering at Pohang University of Science and Technology (POSTECH), Korea. He received his PhD in chemical engineering from KAIST, Korea, in February 2002. He then joined Bell Laboratories, USA, as a postdoctoral researcher in 2002. From September 2003 to August 2008, he worked at the Samsung Advanced Institute of Technology, Samsung Electronics, as a member of research staff. He received a Korea Young Scientist Award from the President of Korea in 2008. He is the author and co-author of 85 papers and 148 patents. His research focuses on printed and organic electronics based on organic and carbon materials for flexible electronics, displays, solid-state lighting and solar energy conversion devices.

O Ok Park is a Professor at the Department of Chemical and Biomolecular Engineering, KAIST, Daejeon, Korea, and he can be reached via ookpark@kaist.ac.kr or 82-42-350-3923. After obtaining PhD at Stanford University in 1985, he has been working at KAIST as a Professor for the last 25 years. His current research interests include polymer solar cells, polymer electroluminescence devices, metal nanoparticles, colloidal self assembly and related nano soft-lithography and polymer nanocomposites. He has published more than 230 papers with more than 3 200 citations. He is a member of both the National Academy of Engineering of Korea and the Korean Academy of Science and Technology.

Although the local vacuum reference energy level is assumed constant at each interface in the organic electronic devices, interface dipoles at organic-metal and organic-organic interfaces are often formed to shift the vacuum levels.[51–53] Interlayers both at the positive and negative electrodes can also influence the energy level alignment at the organic-organic and organic-electrode interfaces.[51–53] For example, the introduction of molecular dipole layers (e.g., self-assembled monolayers) at organic-electrode

interfaces can tune the effective workfunction of the transparent conducting oxides and metals.[53,54] Since most of interlayers can control the effective work function of both the electrodes, the charge extraction from the organic photoactive layers to the electrodes can be effectively controlled.[52,53] In this work, we review recent progress resulting from including interlayers in OPVs.

Interfacial Layers for Efficient Hole Extraction in OPVs

It has been demonstrated that control of the hole and electron extraction in OPVs by modifying the interface between the anode and the active layer plays an important role in improving the device efficiency.[31–36] However, to date, studies on hole extraction layers relative to the electron extraction layer in OPVs have not been conducted actively and are limited. Although introduction of some surface treatments and interfacial dipole layers at the positive electrode have been conducted to improve the device efficiencies,[35,47] only a few papers on new hole extraction layers have been published recently.[32,36] Reviewing the history of the development of OLEDs, the role of hole injection and the buffer layer are very crucial for efficient hole injection, recombination and prolonged device lifetime. Therefore, research along these lines will become much more important as the development of OPVs progresses.

Polymeric Hole Extraction Layers to Improve Hole Extraction

Modification of the interface between the anode and the active layer has been performed mostly to reduce the charge injection/extraction barrier in OLEDs and OPVs. Poly(3,4-ethylenedioxythiophene):poly(styrenesulfonate) (PEDOT:PSS) is a well known conducting polymer that has often been used for the anode buffer and hole extraction layer in OPVs, as well as the hole injection layer in OLEDs. The usual work function of conventional PEDOT:PSS (Baytron PH or Baytron P VP AI4083, H. C. Starck) ranges from 5.0 to 5.2 eV. Since the work function of the PEDOT:PSS films lies between the work function of ITO ($\approx$4.8 eV) and the ionization potentials (IPs) of the donor polymers ($\approx$5.2–5.5 eV), the film can facilitate hole extraction from the photoactive layer. In the case in which the IP of the donor polymer is much higher than the work function of PEDOT:PSS (IP > 5.2 eV), it is necessary to tune the surface work function of PEDOT:PSS. Recent reports demonstrate that the surface work function can be tuned by controlling the surface layer compositions in the PEDOT:PSS films. Figure 1 shows that the surface work function of the PEDOT:PSS film is clearly dependent on the ratio of PSS to PEDOT at the surface. Lee et al. found that
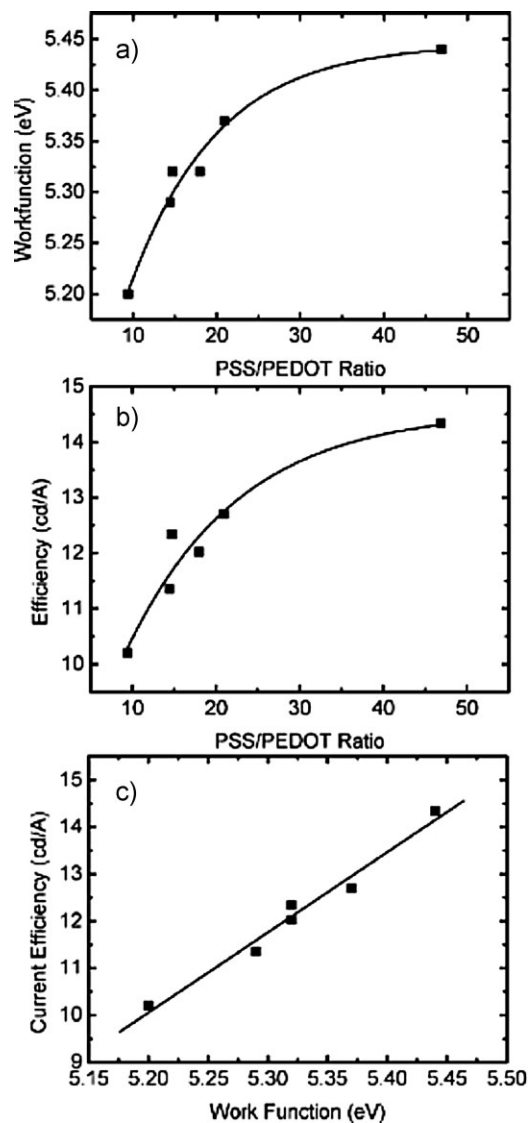

Figure 1. The effects of the ratio of PSS to PEDOT at the film surface on the film work function and the current efficiency of polymer light-emitting diodes using a green-emitting polyfluorene derivative as the emitting layer. Reprinted with permission from ref.[44] © 2009 Wiley-VCH.

the work function of PEDOT:PSS can be increased up to 5.44 eV.[44] The current efficiency in polymer light-emitting diodes using a green emitting polyfluorene derivative as the emitting layer is also dependent on the ratio of PSS to PEDOT at the surface. Similarly, work function tuning of PEDOT:PSS is expected to be employed to improve the power conversion efficiency of OPV devices.

Li et al. incorporated a hole extraction layer, sulfonated poly(diphenylamine) (SPDPA) instead of PEDOT:PSS, in polymer photovoltaic cells.[36] The SPDPA showed a slightly higher work function (5.24 eV) compared to PEDOT:PSS (5.07 eV), which made the hole extraction favorable in the

devices.[36] In addition, a 10 nm thick SPDPA film improved the crystallinity of poly(3-hexylthiophene) (P3HT) and thus the hole mobility was enhanced. As a result, the hole extraction was enhanced, improving the power conversion efficiency. This example shows how hole extraction layers can improve the power conversion efficiency by reducing the hole extraction barriers and improving the hole mobility of the photoactive layers. A thin fluoropolymer layer of polytetrafluoroethylene (PTFE) was also employed as the hole extraction buffer layer in polymer photovoltaic cells by Kang et al.[32] The 1∼5 nm thick PTFE forms an artificial dipole layer resulting from the rich, negatively charged fluorine that facilitates the hole extraction process. However, the authors did not report the surface energy in the paper. Since PTFE containing fluorocarbons usually have very low surface energies (19 mN·m^{-1}), the layer could affect the morphology of the photoactive layers.

As described above, the hole extraction layer should be designed to have a low hole extraction barrier and to induce enhanced crystallinity of the photoactive layer. In this regard, PEDOT:PSS can be modified to have a higher work function and lower surface energy in films, as reported elsewhere.[45] Lee et al. reported that incorporation of a perfluorinated ionomer (PFI) in the PEDOT/PSS film can improve the surface work function of spin-cast films, whose work function was greatly increased from 5.20 eV to 5.5 eV by varying the PFI concentration in the film.[45] Since the layer contains fluorinated carbons, the surface energy of the films will be quite low ($\approx$ 20 mN·m^{-1}), which gives rise to a large surface energy contrast between the hole extraction layer and the photoactive layer, based on P3HT (26.9 mN·m^{-1}):[55] PCBM (38.2 mN·m^{-1}).[56] This arrangement can provide favorable morphology for charge transport via slow drying, solvent annealing or thermal annealing.

Self-assembled Molecules for Surface Treatment of Indium Tin Oxides

The interface between the organic active layers and the anode is important to achieve efficient hole extraction in OPVs. There have been several different surface treatment methods for tuning the effective work function of indium tin oxide (ITO), including the formation of self-assembled dipolar molecules,[35,47,57] deposition of metal oxide layers,[33,34,58,59] various gas plasma treatments[60] and UV ozone treatment.[60] Among them, the formation of self-assembled monolayers (SAMs) on ITO is a well-known approach to control the effective work function in organic light-emitting diodes by shifting the vacuum level.[57] Modification with electronegative molecules can shift the local vacuum level to increase the effective work function, whereas modification with electron-donating molecules lowers the effective work function.[35,47,57] Kim et al. reported that by using SAMs with terminal groups of

−NH$_2$, −CH$_3$ and −CF$_3$, the hole extraction barrier from the P3HT:PCBM blend to ITO can be controlled.[47] Since fluorinated molecules can increase the work function of the ITO, a solar cell device with CF$_3$ SAM-treated ITO was found to exhibit the highest power conversion efficiency.[47] Sharma et al. recently reported the work function tuning of ITO using pentafluorobenzyl phosphonic acid (F5BPA) and 3,3,4,4,5,5,6,6,7,7,8,8,8-tridecafluorooctylphosphonic acid (FOPA) surface modifiers.[35] The use of F5BPA increased the work function to a value of 4.90 eV, 0.4 eV higher than the unmodified ITO. When FOPA was used, the work function increased further to 5.3 eV. However, when the authors deposited pentacene as the donor on top of the ITO, the device power conversion efficiency was not dependent on the work function. The ionization potential (IP) of pentacene is 4.9 eV, which is close to the work function of unmodified ITO ($\approx$4.8 eV). Lack of an effect on device efficiency is attributed to Fermi level pinning at the ITO/pentacene interface. Therefore, incorporation of a donor material with an IP greater than the work function of ITO is necessary to observe the ITO modification effect on hole extraction from the photoactive layer. Khodabakhsh et al. reported that improved hole extraction in OPVs using copper phthalocyanine (CuPc, IP = 5.2 eV) as a donor layer was achieved using self-assembled dipole molecules, such as 4-chlorobenzoylchloride (CBC), 4-chlorobenzenesulfonyl chloride (CBS) and 4-chlorophenyldichlorophosphate (CBP).[61] The improvement was attributed to the lowered hole extraction barrier between ITO and CuPc due to the increased work function of the anode, as well as the improved compatibility of the SAM-modified electrodes with the subsequently deposited organic layers.[61]

Surface treatment of the substrates using self-assembled molecules can also control the phase segregated morphology of the photoactive polymer blend which is also another important aspect of the molecular interlayer to improve device efficiency. The BHJ structure, organized by an efficient interpenetrating donor-acceptor morphology, has been introduced to overcome the low charge carrier mobility of organic materials and the high possibility of recombination, resulting in an increase of the photocurrent density of OPV devices. Generally, OPV devices with a bilayer structure demonstrate a much lower power conversion efficiency, because most of the charge generation and separation occurs only at the interface between two layers with different electron and hole affinities. However, a bilayer device could be more effective to transport the separated holes and electrons at the interface to the electrodes with a much lower possibility of electron-hole recombination compared to the BHJ. One can expect that the gradient morphology may show several positive effects on the cell performance because this concentration graded phase separation morphology will induce not only an charge separation similar to BHJ, but it may also provide

an effective charge transport pathway in the active layer and thus efficient charge collection at the electrodes similar to the bilayer structure. Generally, polymer blends are likely to phase separate when cast from a mixed solution due to the low entropy of mixing. Yang Yang's group investigated the top and bottom surfaces of the polymer active layer and revealed an inhomogeneous concentration of the donor and acceptor materials inside the P3HT/PCBM film.[62] Recently, several groups reported that vertical segregation of the active layer in the P3HT:PCBM blend depends on the surface properties of the substrate.[63] The specific interlayer affects the vertical phase separation behavior. For example, film prepared on a quartz substrate showed a concentration gradient varying from PCBM-rich near the substrate side to P3HT-rich near the air surface. In contrast, when the quartz surface was modified by hydrophobic SAM (hexamethyl-disilazane), the vertical segregation direction was reversed, with P3HT accumulating in the bottom part and PCBM segregation occurring at the air surface. Chen et al. also reported a method for controlling the submicron scale phase separation of P3HT and PCBM in OPVs. When using the microcontact printing method to fabricate patterned 3-aminopropyltriethoxysilane on a PEDOT:PSS layer, an interdigitated structure vertically aligned to the substrate surface was achieved after spontaneous surface directed phase separation.[64] The hole mobility increased as a consequence of improved polymer chain ordering, resulting in a higher device efficiency.

UV Ozone Treatment Effects

UV ozone treatment has been applied to improve the work function of ITO and PEDOT:PSS.[60,65–68] Even following UV ozone treatment on ITO, it is arguable whether the anode surface treatment is effective for hole extraction in the OPVs. Hong et al. reported that, although various gas plasma and UV ozone treatments on ITO affected both the surface energy and work function of the ITO substrates, the series and shunt resistances of the OPV cells did not change significantly.[60] Therefore, the authors concluded that surface treatment of ITO did not make a significant impact on the device performance.[60] However, these treatments have been very effective for organic light-emitting diodes because they can alter the hole injection barrier for efficient hole injection.[60,68] The current flow of the OPV is opposite to that of OLEDs at the ITO/organic contact. It is still important to investigate the hole extraction mechanism at the interface and how the hole extraction will be different from the hole injection at the interface.

The workfunction of PEDOT:PSS increased after UV ozone treatment was applied to PEDOT:PSS films.[66] However, the hole injection barrier to *N,N'*-diphenyl-*N,N'*-bis-(1-naphthyl)-1-1'-biphenyl-4,4'-diamine(α-NPD) increased, resulting in a lower current density in hole-only devices.[66]
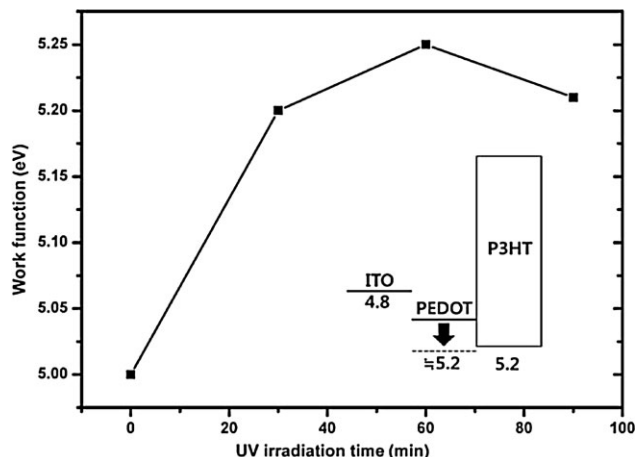
*Figure 2.* The work function of the PEDOT:PSS layer as a function of the UV irradiation time. The inset shows a diagram of the proposed energy level demonstrating the change of the work function of PEDOT:PSS before and after UV irradiation. Reprinted with permission from ref.[67] © 2009 Elsevier B.V.

The apparent increase in the work function of UV ozone-treated PEDOT:PSS is attributed to a metastable surface dipole resulting from the UV ozone treatment.[66] In contrast, Benor et al. reported that the UV ozone treatment decreases the work function of PEDOT:PSS and that the charge balance in OLED devices was enhanced, which resulted in a greatly improved device efficiency.[65] Recently, Lee et al. reported that UV irradiation on PEDOT:PSS increased the work function of the film, as shown in Figure 2, which was measured by the Kelvin probe method.[67] They revealed that the work function can be improved by 0.25 eV after UV irradiation for 1 h.[67] When they used the UV irradiated PEDOT:PSS films as a hole extraction layer, the OPVs showed a greatly improved power conversion efficiency which increased from 3.05 to 3.50%, as shown in Figure 3. This improvement was attributed to the lower series resistance of the devices. The increase of the short circuit current, shown in Figure 3, indicates that the hole extraction from the photoactive layer is enhanced due to the increased work function of the PEDOT:PSS films.

Metal Oxides as an Interfacial Layer for Better Hole Extraction

Metal oxides, such as V_2O_5, MoO_3 and NiO, as opposed to PEDOT:PSS, have been exploited as interfacial hole extraction layers between the positive electrode and the photoactive layer in OPVs.[33,58,69–70] Shrotriya et al. reported the use of the transition metal oxides V_2O_5 and MoO_3 as efficient interfacial buffer layers in polymer photovoltaic cells. Devices with an oxide interfacial layer showed performances similar to or better than devices with
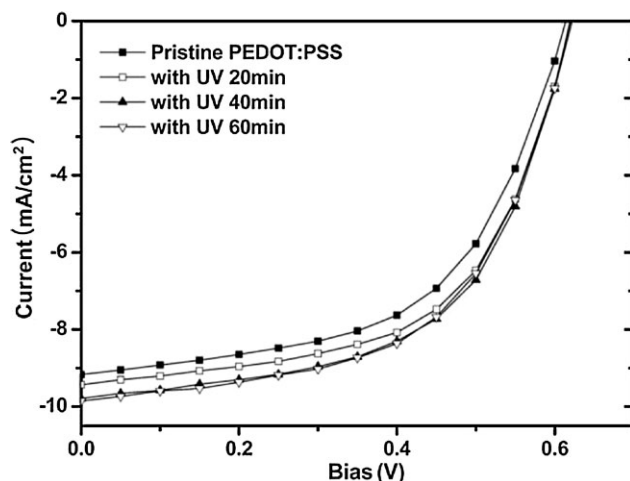
Figure 3. Current-voltage characteristics of PVs with different UV irradiation times on PEDOT:PSS films: pristine PEDOT:PSS (■); with 20 min UV irradiation (□); with 40 min irradiation (▲); with 60 min UV irradiation (△). Reprinted with permission from ref.[67] © 2009 Elsevier B.V.

a PEDOT:PSS layer.[69] A P3HT:PCBM photovoltaic device with a 5 nm thick MoO_3 film as the interfacial buffer layer showed the highest power conversion efficiency of 3.3%, which was slightly greater than that of the OPV device with a PEDO:PSS layer (3.18%).[69] More recently, Kim et al. reported that both vacuum deposited small molecule and solution processed polymer photovoltaic cells with a 10 nm thick MoO_3 interfacial layer showed more pronounced improvements of the power conversion efficiency compared to devices with a PEDOT:PSS buffer layer.[33] The significant improvement of power conversion efficiency was ascribed to an increase of the fill factor and a reduction in the series resistance.[33] Although the power conversion efficiency of the P3HT:PCBM device with the MoO_3 interfacial layer (3.3%) was improved relative to that of the device with the PEODT:PSS layer (2.8%), it is still not the highest value ever observed. Irwin et al. reported a high power conversion efficiency (5.16%) in OPV devices based on a P3HT:PCBM photoactive layer by employing *p*-type semiconducting nickel oxide (NiO) as an interfacial layer.[58] The NiO layer improves the V_{oc} and the fill factor greatly by suppressing OPV interfacial losses and their adverse effects on V_{oc} and the fill factor. This interfacial layer approach can be used to improve hole extraction at the interface between ITO and the polymer active layer.[58] Yoon et al. reported an improved efficiency of up to 4.8% with a high fill factor of 63% for P3HT:PCBM bulk heterojunction photovoltaic devices using ITO positive electrode surface modified via plasma oxidized silver (AgO_x).[59] The short circuit current density of P3HT:PCBM devices using the AgO_x layer was enhanced without significant losses in the V_{oc} (0.6 V) or the fill factor (63%), leading to an efficiency improvement from

4.4% in the control devices to 4.8% for the surface-modified ITO anode.[59] The enhanced short circuit density is attributed to an interface energy step between the ITO and the PEDOT:PSS. The introduction of an interface energy step could alter the hole extraction efficiency, resulting in an improved overall efficiency in OPV devices. The oxide layers mentioned above can play important roles in preventing unwanted chemical reactions between the ITO and the active layer. The lack of reactions is be beneficial to improve the device stability.[58] The acidic nature of PEDOT:PSS is known to etch ITO, after which In and Sn atoms can migrate into the photoactive layer during operation, which may shorten the device lifetime.[45,70] In this regard, the oxide interfacial layer should be studied in depth in the near future to determine the effect of the layer on the device degradation.
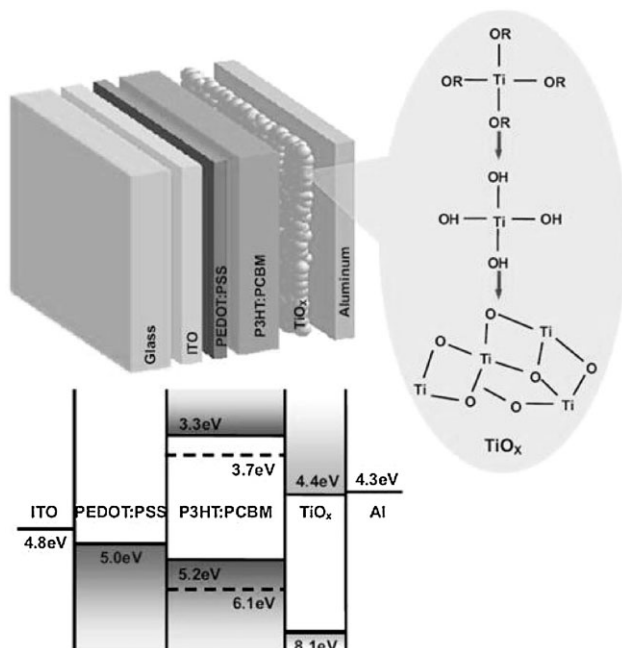
Interfacial Layers for Efficient Electron Extraction in OPVs

As with interlayers for efficient hole extraction from the active layer, several interlayer materials for efficient electron extraction have been reported.[37] However, most conducting polymers do not have a comparable work function with a metal cathode and, therefore, organic materials cannot be adapted as interlayers in OPVs. Recently, several research groups have focused on interfacial materials based on inorganic materials prepared from solution processes or a thermal evaporation method. As a result, the cell performances and stability have been greatly improved due to the unique interlayers in OPVs.

Titanium Oxide Interfacial Layer Between the Active Layer and the Metal Electrode

Titanium oxide (TiO_2) is a popular material for use as an electron acceptor or transport material, as confirmed by its use in dye-sensitized solar cells[71,72] and conjugated polymer/TiO_2 hybrid solar cells.[73–75] Generally, TiO_2 should be treated at a high temperature of over 400 °C to obtain crystallinity and to allow its use in either the anatase or the rutile phase. Sintered TiO_2 nanoparticles were reported to have an electron mobility of $10^{-6}\sim10^{-7}$ $cm^2 \cdot Vs^{-1}$.[76,77] However, it is impossible for polymeric or organic active materials to survive at high temperature.
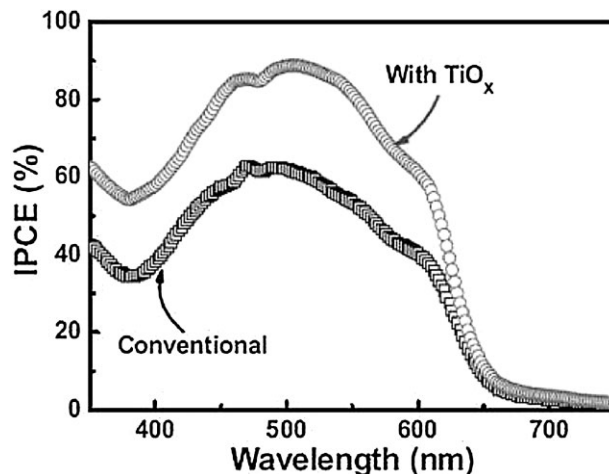
Heeger's group recently used a solution-based sol-gel process to fabricate a TiO_x layer with a thickness of around 30 nm on top of the active layer (Figure 4).[78] The sol-gel procedure used to produce TiO_x involves the following steps. Titanium (IV) isopropoxide (TTIP) was prepared as a precursor and mixed with 2-methoxyethanol and ethanolamine in a three-necked flask equipped with a condenser, a

2100

Macromol. Rapid Commun. **2010**, *31*, 2095–2108

© 2010 WILEY-VCH Verlag GmbH & Co. KGaA, Weinheim

Macromolecular
Journals

DOI: 10.1002/marc.201000310

Figure 4. Schematic illustration of the device structure with a brief flow chart of the steps involved in the preparation of the TiO_x layer. The energy levels of the single components of the photovoltaic cell are also shown. P3HT refers to poly(3-hexylthiophene) and PCBM represents [6,6]-phenyl C61-butyric acid methyl ester. Reprinted with permission from ref.[78] © 2006 Wiley-VCH.

Figure 5. Incident monochromatic photon-to-current collection efficiency spectra for devices with and without the TiO_x optical spacer layer. Reprinted with permission from ref.[78] © 2006 copyright Wiley-VCH.

thermometer and an argon gas inlet/outlet. Then, the mixed solution was heated to 80 °C for 2 h in a silicon oil bath under magnetic stirring, followed by heating to 120 °C for 1 h. The two step heating procedure (80 and 120 °C) was then repeated. The typical TiO_x precursor solution was prepared in isopropyl alcohol.[78] Because the TiO_x layer was treated at a temperature below 100 °C, the film showed an amorphous structure, which was confirmed by X-ray diffraction data. They also investigated the band gap ($\approx$3.7 eV) of the synthesized TiO_x material using UV absorption data and cyclic voltammograms with which the energies of the bottom of the conduction band and the top of the balance band of the TiO_x were defined (Figure 4).

The authors compared the incident photon-to-current collection efficiency (IPCE) spectra of devices fabricated with and without a TiO_x interlayer (Figure 5). The IPCE is defined as the number of photogenerated charge carriers contributing to the photocurrent per number of incident photons. The conventional device showed the typical spectral response of P3HT:PCBM composites with a maximum IPCE of $\approx$60% at 500 nm.[78] For the device with the TiO_x interlayer, the IPCE was substantially enhanced by $\approx$40% over the entire excitation spectral range. The authors explained that these unique effects originated from the increased absorption in the bulk heterojunction layer

owing to the TiO_x optical spacer effect; the increased photogeneration of charge carriers results from the spatial redistribution of the light intensity.

More recently, Heeger's group reported that the internal quantum efficiency is close to 100%, which implies that all absorbed photons result in a separated pair of electron and hole charge carriers. In addition, all photo-generated carriers are collected at each anode and cathode by use of poly[N-9″-hepta-decanyl-2,7-carbazole-alt-5,5-(4′,7′-di-2-thienyl-2′,1′,3′-benzothiadiazole) (PCDTBT)/[6,6]-phenyl C_{70}-butyric acid methyl ester ($PC_{70}BM$) (Figure 6).[79] The device with the TiO_x layer also demonstrated a higher IPCE throughout the visible range, when compared to the device without the TiO_x layer, because of the higher short circuit current of the device with the optical spacer between the incident light and the reflected light from the interface between aluminum and TiO_x.

Yoshikawa's group also reported similar effects of the TiO_x interlayer.[80] Their TiO_x layer was prepared by simply spin coating an ethanol solution of TTIP. The TTIP was hydrolyzed and converted into TiO_x during the spin coating process by contact with water present in the air. They reported the thickness effects of TiO_x on three important factors and the PCE. The efficiency of cells without the TiO_x layer was in the range of 1.4% to 2.0% while the efficiency of the cell with a 5~11 nm thick TiO_x layer showed a maximum efficiency value of approximately 4%. Thicker TiO_x layers led to lower efficiencies, due to the increased series resistance. V_{oc} and FF dramatically increased from 0.4 to 0.6 V and from 0.5 to 0.7 V, respectively, whereas I_{sc} only slightly increased when thicker TiO_x layers were used.

Li's group also applied another type of Ti-based precursor, a solution processable titanium chelate, titanium (diiso-
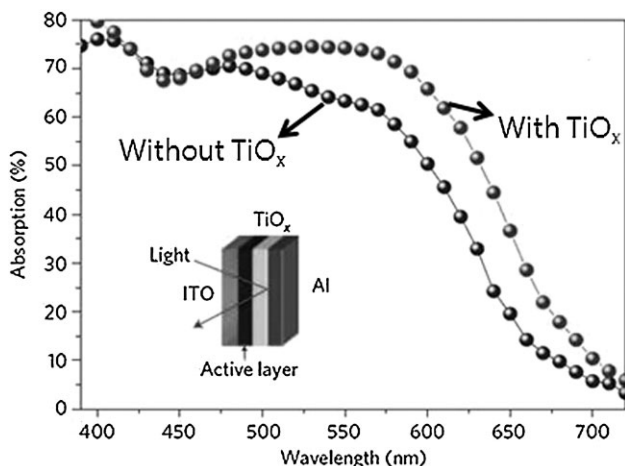
Figure 6. The effects of using a TiO$_x$ layer as an optical spacer on the device performance where the total absorption in the active layer was measured in reflection geometry with the TiO$_x$ layer and without the TiO$_x$ layer. The inset shows a schematic of the device structure. Reprinted with permission from ref.[79] © 2009 Nature Publishing Group.

Figure 7. AC impedance plots of the devices with and without a TIPD cathode buffer layer in the dark at 0 V. The inset shows an equivalent RC circuit of the PSCs in the dark. Reprinted with permission from ref.[81] © 2007 American Institute of Physics.

propoxide) bis (2,4-pentanedionate) (TIPD), as the cathode buffer layer in solar cells based on a blend of poly[2-methoxy-5-(2′-ethylhexyloxy)-1,4-phenylenevinylene] (MEH-PPV) and PCBM.[81] The TIPD layer was spin coated from an isopropanol solution on the active layer and then dried at 70 °C for 30 min. Figure 7 shows the ac impedance plots for the devices at 0 V in the frequency range of 10 ~1 MHz. The impedance plots show standard semi-circles, which represent the general behavior of the polymer light-emitting diodes. Li's group proposed an equivalent circuit of resistance and capacitance in parallel, as shown in the inset of Figure 7. The resistance, *R,* can be obtained from the diameter of the semicircle on the "Re" axis. The *R* of the device without TIPD was about 19 kΩ, while that the resistance of the device with TIPD decreased dramatically to 10.8 kΩ. From the impedance results, the authors insisted that the TIPD buffer layer reduced the interface resistance between the active layer and Al electrode, leading to a lower device resistance. The PCE of the solar cell with a TIPD buffer layer was 2.52%, which is an increase of 51.8%, when compared to the device without the TIPD buffer layer (PCE of 1.66%) under the same experimental conditions.

Park's group recently discovered that a TiO$_x$ interlayer plays another important role in devices with an Al electrode deposited at a low vacuum pressure.[82] As shown in Figure 8, as the vacuum pressure was increased, the performance of the device decreased. Among the three factors involved in the calculation of PCE, J_{sc} critically decreased the efficiency of the devices. The J_{sc} of the device with the TiO$_x$ layer decreased from 9.60 mA·cm^{-2} to 7.27 mA·cm^{-2}. However, the efficiency of the device with the
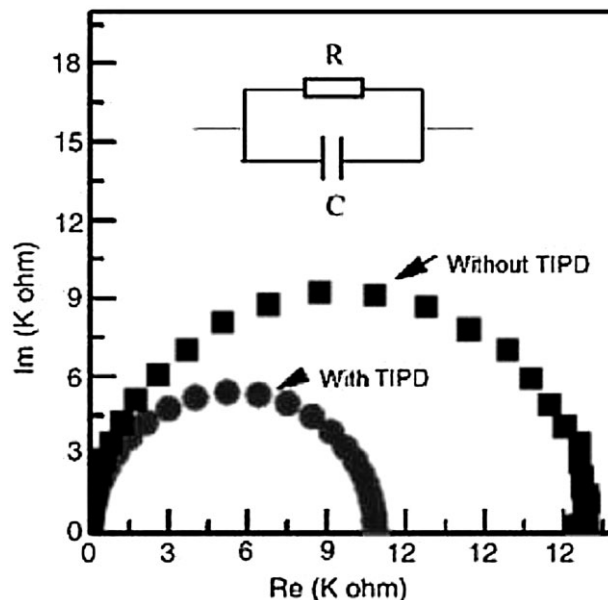
TiO$_x$ layer is less dependent on the vacuum pressure during Al deposition. From the above results, they concluded that that interfacial effect, which is degraded by the rough surface of the Al electrode deposited at a low vacuum pressure, may be overcome by inserting a TiO$_x$ layer between the active layer and the Al electrode.

While the reported cell PCEs are close to fulfilling some of the requirements for commercial application, the long term stability of OPVs is still an obstacle to overcome before their commercialization.[83] In order to achieve a better device lifetime of photovoltaic devices, attempts to create encapsulation using organic/inorganic hybrid multilayer barriers with a total thickness of several micrometers have been reported with promising results. However, in most cases such a process requires glass substrates or expensive multilayer barrier films.[84] Despite the remarkable improvements in the long term stability obtained with encapsulation technology, most of these devices exhibit poor flexibility and a significantly increased fabrication cost.

Numerous research groups have recently reported OPVs with a TiO$_x$ interlayer between the active layer and the Al electrode. The K. Lee and Alan J. Heeger groups reported air stable polymer solar cells fabricated by an all solution processing technique using a TiO$_x$ interlayer as a shielding and scavenging layer, which prevents the intrusion of oxygen and humidity into the electronically active polymers.[49] The inserted TiO$_x$ layer improves the lifetime of the polymer-based solar cells. As can be seen in Figure 9, when
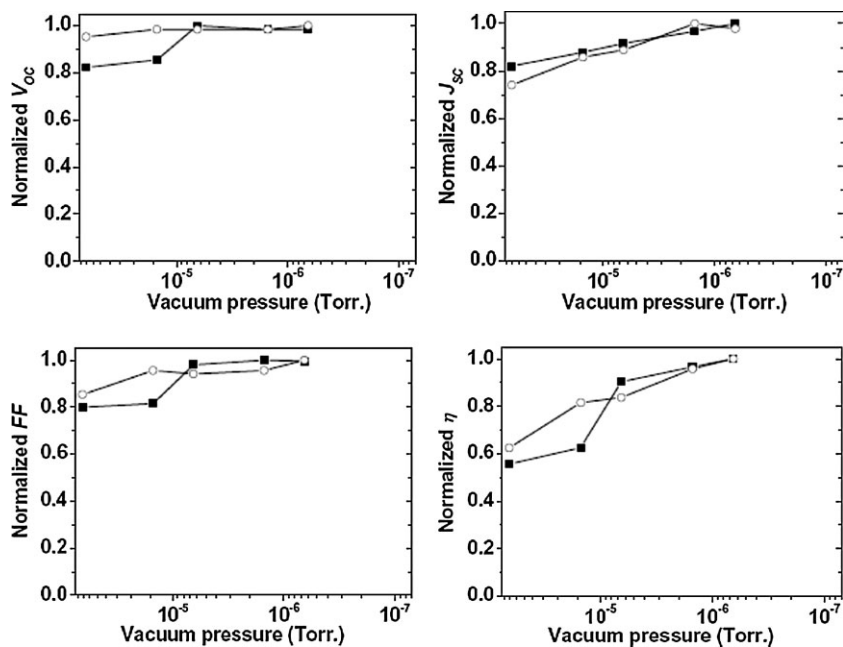
Figure 8. Normalized values of V_{oc}, J_{sc} and FF, and efficiency of the reference devices (■) and the devices with a TiO$_x$ layer (○) fabricated at various vacuum pressures. Reprinted with permission from ref.[82] © 2007 American Institute of Physics.

only 0.94 in 100 h, whereas the J_{sc} of the device without TiO$_x$ decreased to approximately 0 (see Figure 10).[80] The efficiencies of organic solar cells lacking a TiO$_x$ layer decreased to 0% after being stored under atmospheric conditions, while, after 50 h, the efficiencies of the cells kept under an Ar atmosphere were reduced to half their initial efficiencies. This information provides evidence of the positive effect of the TiO$_x$ layer blocking oxygen invasion into the active layer.

However, in the case of a device with a TiO$_x$ interlayer prepared from TTIP, the most widely used precursor, the high temperature long term stability was worse than that of the neat device (without a TiO$_x$ interlayer). This indicates that devices with a TiO$_x$ interlayer are not stable when operated under high temperature conditions. For this reason, other recently introduced devices with a TiO$_x$ interlayer have not been annealed at high temperatures after coating the Ti precursor on the active layer during cell preparation.[80–82] The explanation for this behavior was provided by Park's group who utilized AFM in their analysis.[50] Obvious morphological changes of the TTIP-based TiO$_x$ interlayer were observed after annealing at high temperature, which possibly deteriorated the interface between Al and the active layer. Hence, they prepared a new precursor solution for the TiO$_x$ interlayer and reported excellent long term, high temperature stability, compared to devices with a TTIP-based TiO$_x$ interlayer (see Figure 11). They referred to this material as polymeric type TiO$_x$.[50]

Recently, the positive effects of a TiO$_x$ interlayer on cell efficiency were confirmed by several groups. However, the

these conventional devices were stored in ambient air, a dramatic decrease of J_{sc} was observed as the storage time increased. However, the decay of the device efficiency of the devices with a TiO$_x$ interlayer was very small, indicating that the devices still function properly without catastrophic failure.

Yoshikawa's group also reported the positive effects of a TiO$_x$ interlayer on the cell stability of polymer solar cells. The J_{sc} of the device containing a TiO$_x$ layer decreased to
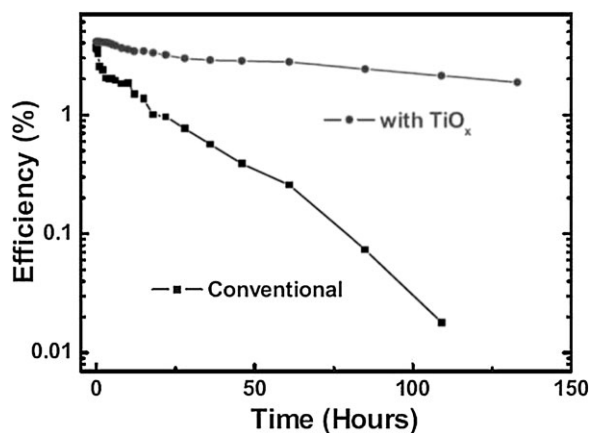

Figure 9. Comparison of the power conversion efficiencies as a function of storage time for polymer solar cells with and without a TiO$_x$ layer. Note that the characteristics of the devices were monitored with increasing storage time. Reprinted with permission from ref.[49] © 2007 Wiley-VCH.
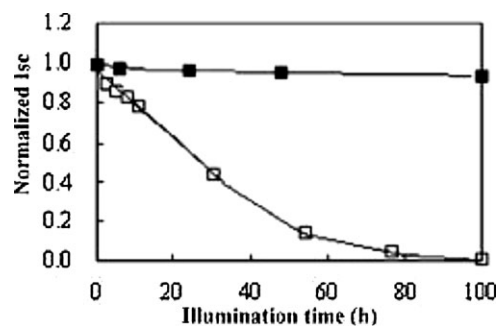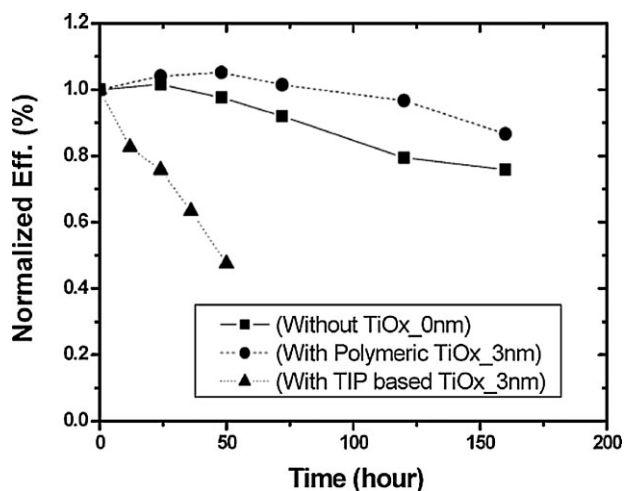

Figure 10. Normalized short circuit current density of devices with (closed square) and without (open square) a TiO$_x$ layer vs. illumination time at AM 1.5, 100 mW · cm^{-2}. Reprinted with permission from ref.[80] © 2007 American Institute of Physics.
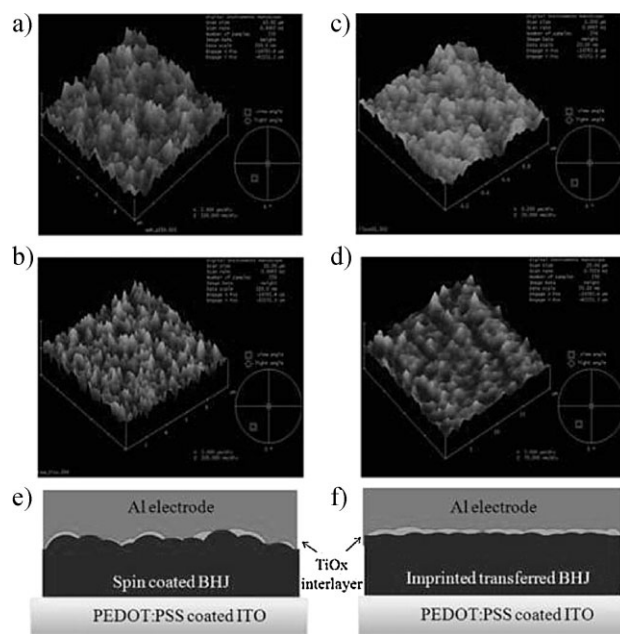
Figure 11. Normalized efficiencies of the devices without TiO$_x$ interlayer, with a polymeric TiO$_x$ interlayer and with TTIP based TiO$_x$ interlayer as a function of the storage time in air at 80 °C. Reprinted with permission from ref.[50] © 2009 American Chemical Society.

Figure 12. (a) AFM 3D images of the spin-coated BHJ, (b) AFM 3D images of the spin-coated BHJ with TiO$_x$ interlayer, (c) AFM 3D images of the imprinted transferred BHJ using UV-curable resin-coated polycarbonate film, (d) AFM 3D images of the imprinted transferred BHJ with TiO$_x$ interlayer using UV curable resin-coated polycarbonate film, (e) whole device sequential inner structure of spin-coated BHJ with TiO$_x$ interlayer on the PEDOT:PSS-coated ITO, and (f) whole device sequential inner structure of imprinted transferred BHJ with TiO$_x$ interlayer on the PEDOT:PSS-coated ITO. Reprinted with permission from ref.[85] © 2010 Elsevier B.V.

cell efficiency was strongly dependent on the thickness of the TiO$_x$ interlayer. From the results obtained by Yoshikawa's group, the conductivity of a 50 nm thick TiO$_x$ film was 1/5th the value of a 10 nm thick TiO$_x$ film. From the results reported by two different groups, the optimum thickness of the TiO$_x$ layer was between 3 and 5 nm.[50,80]

Recently, several groups have been trying to prepare an active layer of OPVs through a stamping technique using a UV-curable resin-coated polycarbonate (UV-PC) film, as well as a polydimethylsiloxane (PDMS) mold.[85] The active layer prepared from the stamping transfer method has a smoother surface morphology, which was confirmed by AFM analysis. Therefore, as shown in Figure 12, stamping the transferred flat surface of BHJ would facilitate the formation of a more uniform thickness of the TiO$_x$ interlayer, which can maximize the device performance. This uniform surface morphology of the active layer prepared from the transfer by stamping technique can result in more positive effects when the technique is combined with the TiO$_x$ interlayer system.

Use of Metal Fluoride Layers for the Negative Electrode Contact in OPVs

As in OLEDs, LiF/Al is a commonly used negative electrode in OPVs. As an interfacial layer material between the active polymer (PCBM) and the metal cathode (Al), the thickness of LiF is limited to less than 1 nm, since thicker layers were determined to be unfavorable for efficient electron collection. The formation of dipoles at the LiF interfacial layer was reported, so that control of the work function of the

negative electrode contact is evident both in OLEDs and OPVs. While the improved performance of OLEDs with LiF has been explained by the formation of AlF$_3$, doping of LiF into the organic layer (dissociation of LiF) and the effect of LUMO level alignment by the tunneling and reduction of the gap state, the major and the role of the LiF has been suggested to be to prevent the reaction between Al and PCBM.[86] Although cathode diffusion into the polymer may not occur or at least is not severe during thermal deposition of aluminum on PCBM, small but non-negligible aluminum diffusion into the active layer during annealing was observed by SIMS.[87] However, in a different metal/organic interface system, strong inter-diffusion of Au/diindenophrylene/silicon oxide heterojunction was observed at high temperature and a low deposition rate. The Au contact prepared at −120 °C and 23 Å · min^{-1} exhibited quite well defined interfaces.[88] Therefore, metal diffusion into the organic layer is strongly dependent on the process conditions (temperature and rate of deposition), and this dependence explains the power conversion efficiency behavior of OPVs produced with various annealing temperatures and aluminum deposition rates. Table 1

Table 1. Device performance of OPV at different Al deposition rates and annealing conditions.

	No annealing	120 °C	150 °C	180 °C	200 °C
Devices with lower rate of Al deposition	1.60% 6.75 mA·cm^{-2} 0.38 (FF) 0.62 V (V_{oc})	2.80% 9.81 mA·cm^{-2} 0.45 (FF) 0.62 V (V_{oc})	2.44% 9.60 mA·cm^{-2} 0.42 (FF) 0.60 V (V_{oc})	2.39% 9.98 mA·cm^{-2} 0.39 (FF) 0.59 V (V_{oc})	2.09% 9.96 mA·cm^{-2} 0.38 (FF) 0.53 V (V_{oc})
Devices with higher rate of Al deposition	1.74% 6.60 mA·cm^{-2} 0.40 (FF) 0.66 V (V_{oc})	2.58% 9.91 mA·cm^{-2} 0.42 (FF) 0.61 V (V_{oc})	2.51% 9.74 mA·cm^{-2} 0.43 (FF) 0.60 V (V_{oc})	2.64% 9.90 mA·cm^{-2} 0.43 (FF) 0.60 V (V_{oc})	2.73% 9.96 mA·cm^{-2} 0.46 (FF) 0.60 V (V_{oc})

summarizes the power conversion efficiencies, short circuit currents, and fill factors of OPVs with ITO/PEDOT:PSS (35 nm)/P3HT:PCBM (1:0.6, 80nm)/LiF/Al. Devices with lower Al deposition rates were prepared with an Al contact of 0.5 Å·s^{-1} in the first 300 Å of deposition, while the higher Al deposition rate was set at 5.0 Å·s^{-1} for the entire 1 500Å deposition process. The data for devices with lower Al deposition rates showed decreased fill factors and V_{oc} values at higher thermal annealing temperatures.

A linear relationship between the V_{oc} and work function of metals (Ca, Ag, Al and Au) has been reported.[89] One earlier study[90] revealed that variation in the V_{oc} was less than 200 mV when using Ca, Ag, Al and Au as the cathode contact. At the appropriate thickness, there seems to be little LUMO level offset between the LiF/Al electrode and PCBM. These phenomena can be explained by the Fermi level pinning of LiF, which is close to that of the LUMO of PCBM. The best performance among several high work function metal electrodes in OPVs was obtained with of LiF/Al.[91]

Other metal fluorides, including NaF, KF and CsF, have been investigated as interfacial layer materials between PCBM and Al contact, exhibiting improved performance in terms of the power conversion efficiency. Compared to LiF, NaF exhibited an improved efficiency, fill factor and V_{oc} with an ultrathin layer thickness (<0.2 nm).[92] The power conversion efficiency of OPVs with the structure MDMO-PPV/PCBM/CsF/Al were higher, when compared to those with a LiF/Al negative electrode.[93] These results could be explained by the lower series resistance of CsF, which is almost constant in the range of the CsF thicknesses studied.[88] Poly(ethylene oxide) (PEO) and conjugated polyelectrolytes were also effective as the interlayer between the active layer and the cathode.[94,95] All these dipole layers influence the energy level alignment at organic-metal interfaces and thereby reduce the effective work function of the negative electrodes.[52] The accumulation of charge carriers at the interface gives rise to a diffusion current, which must be compensated for with a drift current at the open circuit, thereby contributing to the scaling of V_{oc} with the work function of cathodes in the case of non-ohmic contact.[96,97]

Organic/Metallic Bilayers for the Negative Electrode Contact in OPVs

A thin organic interfacial layer of BCP (2,9-dimethyl-4,7-diphenyl-1,10-phenanthroline) has been employed in OPVs with an ITO/PEDOT:PSS/CuPc/C60 structure with aluminum or Ag electrodes.[98–100] An improved power conversion efficiency when using BCP at the interface between C60 and the metallic electrode is reflected in the enhanced open-circuit voltage from 0.70 to 0.92 V. The optimum thickness for the passivation on C60 with BCP was found to be around 10 nm, while thicker films are disadvantageous for effective charge collection at the negative electrode contact.

Recently, there have been many reports of new electron transport materials employed in phosphorescent OLEDs, which result in a reduction of the driving voltage.[100] A spirobenzofluorene-based phosphine oxide interlayer and 2,7-bis(diphenylphosphoryl) spiro[fluorene-7,11'-benzo-fluorene] (SPPO21) were found to be effective as interfacial buffers for negative electrodes in OPVs.[101] The protection of the active layer from Al deposition and interfacial band bending is the possible mechanism of the high electron mobility of the organic interfacial layer, which will be beneficial for the improvement of OPV cell performance by providing more flexibility in the control of thickness. For the bulk-heterojunction type polymeric OPVs, the effects of the organic interfacial layers on the open circuit voltage and power conversion efficiency have not been extensively investigated.

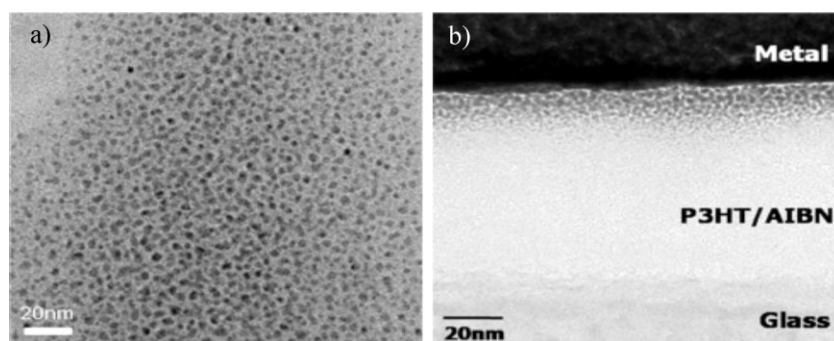**Efficient Hole or Electron Extraction via Nano-patterned Structure in OPVs**

The formation of an interpenetrated structure between the active layer and the electrode can enhance the PCE of OPVs. Park's group recently reported P3HT/PCBM BHJ organic solar cells fabricated on highly ordered 2D-dot nano-patterned anodes prepared by a simple nano-imprinting process.[102] The highly ordered 2D-dot nano-patterned anode can enhance the device performance because of the increased interfacial contact area between both of the
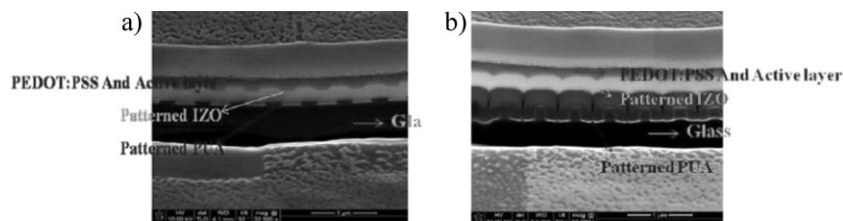
Figure 13. FIB (Focused Ion Beam) tilted images (a) whole device sequential inner structure of PUA (height 50 nm) patterned with IZO, spin coated with PEDOT:PSS and an active layer (P3HT:PCBM) (b) whole device sequential inner structure of PUA (height 200 nm) patterned with IZO, spin coated with PEDOT:PSS and an active layer (P3HT:PCBM). Reprinted with permission from ref.[102] © 2010 Elsevier B.V.

electrodes and the BHJ active layer (Figure 13). This means that the nano-patterned structures play an important role of efficiently harvesting electrons and holes from the active layer to each electrode. Even though enhanced optical absorption is realized due to light trapping or scattering of reflected light by the nano-pattern, the enhanced photo-currents were not fully explained by these two factors. The researchers proposed that the enhancement was also due to the increased contact area, which can assist electron and/or hole extractions. Very similar observations and explanations were reported by Jung's group. They also reported enhanced solar cell efficiency with the formation of nanopores on the active layer prepared from commercially available anodic aluminum oxide (AAO) membrane filters.[103] This control of the contact between the active layer and the metal cathode can increase the effective light scattering, resulting in a great utilization of incident light in the device. The control can also decrease the number of dead ends in the PCBM phases and yield an improved crystalline ordered structure of the P3HT domain, which results in a higher J_{sc} value with increased electron transportation. Na et al. also reported similar observations after controlling the interface between the active layer and the metal cathode. Their method was developed from the simple soft lithography method.[104]

Additionally, it was demonstrated that by adding the thermal initiator 2,2′-azobisisobutyronitrile (AIBN) as a nano-hole generating agent into the BHJ active layer to broaden the contact area with a simple and nonlithographic approach, organic/metal interfaces are created.[105] The AIBN releases nitrogen gas after absorbing thermal energy from the active layer surface, greatly increasing the interfacial area, as shown in the cross-sectional TEM images in Figure 14. The device performance was enhanced by facilitated charge collection via reduced contact resistance and a shortened path-

way to the electrode as a consequence of the enlarged interface area.

Conclusion and Remarks

In this review, we provided an overview of several positive effects of interfacial layers, such as hole extraction and electron extraction layers located at the interface between the photo-responsive active layers and electrodes, resulting in not only improvement of the solar-to-electricity conversion efficiency, but also the long term device stability. In the OPV research field, research concerned with device design through effective interfacial layers has not yet been well developed. Most research papers, in fact more than 70% of those published within the past five years, as determined from the ISI web of knowledge database, have addressed active layer materials or active layer morphologies. As seen in the results of several research papers introduced in the above sections, the efficiencies of OPVs can be varied due to interfacial layers between the active layer and electrode, even though the devices were prepared with the same active materials and morphologies. Moreover, we summarized the crucial positive effects of interlayers from past results in the OLED research field. We believe that the present review can stimulate further research in this emerging topic for enhancing cell performance and stability. In the last section, we also introduced the importance of controlling the interface between the active layers and electrodes. We believe that the optimization of the active layer-electrode nanostructure by surface morphology control may be one method to enhance the light harvest efficiency in OPVs. Many researchers have tried to fabricate a nanopatterned bilayer heterojunction cell or a nanopatterned interface between the BHJ and an electrode, and several positive

Figure 14. TEM images of P3HT/AIBN = 1:0.1 film after heating at 105 °C for 5 min. (a) In plane. (b) Cross-section. Reprinted with permission from ref.[105] © 2010 American Institute of Physics.

effects have been observed. It is hoped that the research field will grow and generate additional beneficial results, as in the field of OLEDs. These approaches may help to achieve a cell efficiency of more than 10% in the near future.

[1] A. J. Heeger, *Angew. Chem., Int. Ed.* **2001**, *40*, 2591.
[2] K. M. Coakley, M. D. McGehee, *Chem. Mater.* **2004**, *16*, 4533.
[3] C. Winder, N. S. Sariciftci, *J. Mater. Chem.* **2004**, *14*, 1077.
[4] S. Gunes, H. Neugebauer, N. S. Sariciftci, *Chem. Rev.* **2007**, *107*, 1324.
[5] E. Bundgaad, F. C. Krebs, *Sol. Energy Mater. Sol Cells* **2007**, *91*, 954.
[6] B. C. Thompson, J. M. Frechet, *J. Angew. Chem. Rev.* **2008**, *47*, 58.
[7] G. Li, Y. Yao, H. Yang, V. Shrotriya, G. Yang, Y. Yang, *Adv. Funct. Mater.* **2007**, *17*, 1636.
[8] G. Yu, J. Gao, J. C. Hummelen, F. Wudl, A. J. Heeger, *Science* **1995**, *270*, 1789.
[9] W. Ma, C. Yang, X. Gong, K. Lee, A. J. Heeger, *Adv. Funct. Mater.* **2005**, *15*, 1617.
[10] G. Li, V. Shrotriya, J. Huang, Y. Yao, T. Moriarty, K. Emery, Y. Yang, *Nat. Mater.* **2005**, *4*, 864.
[11] P. Schilinsky, U. Asawapirom, U. Scherf, M. Biele, C. J. Brabec, *Chem. Mater.* **2005**, *17*, 2175.
[12] K. Kim, J. Liu, M. A. G. Namboothiry, D. L. Carroll, *Appl. Phys. Lett.* **2007**, *90*, 163511.
[13] K. C. Kim, J. H. Park, O. O. Park, *Sol. Energy Mater. Sol Cells* **2008**, *92*, 1188.
[14] F. Paninger, R. S. Rittberger, N. S. Sariciftci, *Adv. Funct. Mater.* **2003**, *13*, 85.
[15] V. D. Mihailetchi, H. Xie, B. de Boer, L. J. A. Koster, P. W. M. Blom, *Adv. Funct. Mater.* **2006**, *16*, 699.
[16] S. H. Chan, Y. S. Hsiao, L. I. Hung, G. W. Hwang, H. L. Chen, C. Ting, C. P. Chen, *Macromolecules* **2010**, *43*, 3399.
[17] L. Li, H. Tang, H. Wu, G. Lu, X. Yang, *Org. Electron.* **2009**, *10*, 1334.
[18] K. Kawano, J. Sakai, M. Yahiro, C. Adachi, *Sol. Energy Mater. Sol. Cells* **2009**, *93*, 514.
[19] H. J. Kim, H. H. Lee, J. J. Kim, *Macromol. Rapid Commun.* **2009**, *30*, 1269.
[20] S. Cho, K. Lee, J. Yuen, G. Wang, D. Moses, A. J. Heeger, M. Surin, R. Lazzaroni, *J. Appl. Phys.* **2006**, *100*, 114503.
[21] Y. Zhao, Z. Xie, Y. Qu, Y. Geng, L. Wang, *Appl. Phys. Lett.* **2007**, *90*, 043504.
[22] J. J. M. Halls, A. C. Arias, J. D. MacKenzie, W. Wu, M. Inbasekaran, E. P. Woo, R. H. Friend, *Adv. Mater.* **2000**, *12*, 498.
[23] A. C. Arias, *Macromolecules* **2001**, *34*, 6005.
[24] S. E. Shaheen, C. J. Brabec, N. S. Sariciftci, F. Padinger, T. Fromherz, J. C. Hummelen, *Appl. Phys. Lett.* **2001**, *78*, 841.
[25] T.-W. Lee, O. O. Park, *Adv. Mater.* **2000**, *12*, 801.
[26] J. Jo, S.-I. Na, S.-S. Kim, T.-W. Lee, Y. Chung, S.-J. Kang, D. Vak, D.-Y. Kim, *Adv. Funct. Mater.* **2009**, *19*, 2398.
[27] J. K. Lee, W. L. Ma, C. J. Brabec, J. Yuen, J. S. Moon, J. Y. Kim, K. Lee, G. C. Bazan, A. J. Heeger, *J. Am. Chem. Soc.* **2008**, *130*, 3619.
[28] D. H. Wang, D. G. Choi, O. O. Park, J. H. Park, *J. Mater. Chem.* **2010**, in press.
[29] D. H. Wang, D. G. Choi, K. J. Lee, O. O. Park, J. H. Park, *Langmuir.* **2010**, DOI: 10.1021 / la100164k.
[30] D. H. Wang, H. K. Lee, D. G. Choi, J. H. Park, O. O. Park, *Appl. Phys. Lett.* **2009**, *95*, 043505.
[31] W.-J. Yoon, P. R. Berger, *Appl. Phys. Lett.* **2008**, *92*, 013306.
[32] B. Kang, L. W. Tan, S. R. P. Silva, *Appl. Phys. Lett.* **2008**, *93*, 133302.
[33] D. Y. Kim, J. Subbiah, G. Sarasqueta, F. So, H. D. Irfan, Y. Gao, *Appl. Phys. Lett.* **2009**, *95*, 093304.
[34] L. Cattin, F. Dahou, Y. Lare, M. Morsli, R. Tricot, S. Houari, A. Mokrani, K. Jondo, A. Khelil, K. Napo, J. C. Bernède, *J. Appl. Phys.* **2009**, *105*, 034507.
[35] A. Sharma, A. Haldi, W. J Potscavage, Jr., P. J. Hotchkiss, S. R. Marder, B. Kippelen, *J. Mater. Chem.* **2009**, *19*, 5298.
[36] C.-Y. Li, T.-C. Wen, T.-F. Guo, *J. Mater. Chem.* **2008**, *18*, 4478.
[37] T.-W. Lee, K.-G. Lim, D.-H. Kim, *Electron. Mater. Lett.* **2010**, *6*, 41.
[38] T.-W. Lee, O. O. Park, *Appl. Phys. Lett.* **2000**, *76*, 3161.
[39] T.-W. Lee, O. O. Park, L.-M. Do, T. Zyung, T. Ahn, H.-K. Shim, *J. Appl. Phys.* **2001**, *90*, 2128.
[40] T.-W. Lee, O. O. Park, *Adv. Mater.* **2001**, *13*, 1274.
[41] T.-W. Lee, H.-C. Lee, O. O. Park, *Appl. Phys. Lett.* **2002**, *81*, 214.
[42] S.-H. Oh, D. Vak, S.-I. Na, T.-W. Lee, D.-Y. Kim, *Adv. Mater.* **2008**, *20*, 1624.
[43] T.-W. Lee, M.-G. Kim, S. H. Park, S. Y. Kim, O. Kwon, T. Noh, T.-L. Choi, J. H. Park, B. D. Chin, *Adv. Funct. Mater.* **2009**, *19*, 1863.
[44] T.-W. Lee, Y. Chung, *Adv. Funct. Mater.* **2008**, *18*, 2246.
[45] T.-W. Lee, Y. Chung, O. Kwon, J.-J. Park, *Adv. Funct. Mater.* **2008**, *18*, 2246.
[46] Y. Liang, Z. Xu, J. Xia, S.-T. Tsai, Y. Wu, G. Li, C. Ray, L. Yu, *Adv. Mater.* **2010**, DOI: 10.1002/adma.200903528.
[47] J. S. Kim, J. H. Park, J. H. Lee, J. Jo, D.-Y. Kim, K. Cho, *Appl. Phys. Lett.* **2007**, *91*, 112111.
[48] M. Ichikawa, C. Shimizu, T. Koyama, Y. Taniguchi, *Phys. Stat. Sol.* **2008**, *205*, 1222.
[49] K. Lee, J. Y. Kim, S. H. Park, S. H. Kim, S. Cho, A. J. Heeger, *Adv. Mater.* **2007**, *19*, 2445.
[50] D. H. Wang, S. H. Im, H. K. Lee, J. H. Park, O Ok Park, *J. Phys. Chem. C* **2009**, *113*, 17268.
[51] J. Hwang, A. Wan, A. Kahn, *Mater. Sci. Engineer.* **2009**, *64*, 1.
[52] S. Braun, W. R. Salaneck, M. Fahlman, *Adv. Mater.* **2009**, *21*, 1450.

[53] N. R. Armstrong, P. A. Veneman, E. Ratcliff, D. Placencia, M. Brumbach, *Acc. Chem. Res.* **2009**, *42*, 1748.

[54] H.-L. Yip, S. K. Hau, N. S. Baek, H. Ma, A. K.-Y. Jen, *Adv. Mater.* **2008**, *20*, 2376.

[55] X. Wang, T. Ederth, O. Ingannäs, *Langmuir* **2006**, *22*, 9287.

[56] C. M. Björström, A. Bernasik, J. Rysz, A. Budkowski, S. Nilsson, M. Svensson, M. R. Andersson, K. O. Magnusson, E. Moons, *J. Phys.: Condens. Matter* **2005**, *17*, L529.

[57] B. de Boer, A. Hadipour, M. M. Mandoc, T. van Woudenbergh, P. W. M. Blom, *Adv. Mater.* **2005**, *17*, 621.

[58] M. D. Irwin, D. B. Buchholz, A. W. Hains, R. P. H. Chang, T. J. Marks, *PNAS*, **2008**, *105*, 2783.

[59] W.-J. Yoon, P. R. Berger, *Appl. Phys. Lett.* **2008**, *92*, 013306.

[60] Z. R. Hong, C. J. Liang, X. Y. Sun, X. T. Zeng, *J. Appl. Phys.* **2006**, *100*, 093711.

[61] S. Khodabakhsh, B. M. Sanderson, J. Nelson, T. S. Jones, *Adv. Funct. Mater.* **2006**, *16*, 95.

[62] Y. Yao, J. H. Hou, Z. Xu, G. Li, Y. Yang, *Adv. Funct. Mater.* **2008**, *18*, 1783.

[63] M. Campoy-Quiles, T. Ferenczi, T. Agostinelli, P. G. Etchegoin, Y. Kim, T. D. Anthopoulos, P. N. Stavrinou, D. D. C. Bradley, J. Nelson, *Nature Mater.* **2008**, *7*, 158.

[64] F. C. Chen, Y. K. Lin, C. J. Ko, *Appl. Phys. Lett.* **2008**, *92*, 023307.

[65] A. Benor, S. Takizawa, P. Chen, C. Pérez-Bolívar, P. Anzenbacher, Jr., *Appl. Phys. Lett.* **2009**, *94*, 193301.

[66] M. G. Helander, Z. B. Wang, M. T. Greiner, Z. W. Liu, K. Lian, Z. H. Lub, *Appl. Phys. Lett.* **2009**, *95*, 173302.

[67] H. K. Lee, J.-K. Kim, O. O. Park, *Organic Electron.* **2009**, *10*, 1641.

[68] J. S. Kim, M. Granström, R. H. Friend, N. Johansson, W. R. Salaneck, R. Daik, W. J. Feast, F. Cacialli, *J. Appl. Phys.* **1998**, *84*, 6859.

[69] V. Shrotriya, G. Li, Y. Yao, C.-W. Chu, Y. Yang, *Appl. Phys. Lett.* **2006**, *88*, 073508.

[70] M. P. de Jong, L. J. van IJendoorn, M. J. A. de Voigt, *Appl. Phys. Lett.* **2000**, *77*, 2255.

[71] B. O'Regan, M. Grätzel, *Nature* **1991**, *353*, 737.

[72] U. Bach, D. Lupo, P. Comte, J. E. Moser, F. Weissörtel, J. Salbeck, H. Spreitzer, M. Grätzel, *Nature* **1998**, *395*, 583.

[73] A. C. Arango, L. R. Johnson, V. N. Bliznyuk, Z. Schlesinger, S. A. Carter, H. H. Horhold, *Adv. Mater.* **2000**, *12*, 1689.

[74] P. A. van Hal, M. M. Wienk, J. M. Kroon, W. J. H. Werhees, L. H. Slooff, W. J. H. Gennip, P. Jonkheijm, R. A. J. Janssen, *Adv. Mater.* **2003**, *15*, 118.

[75] H. Hansel, H. Zettl, G. Krausch, R. Kisselev, M. Thelakkat, H. W. Schmidt, *Adv. Mater.* **2003**, *15*, 2056.

[76] B. O. Aduda, P. Ravirajan, K. L. Choy, J. Nelson, *Internat. J. Photoenergy* **2004**, *6*, 141.

[77] C. J. Brinker, G. W. Scherer, *Sol-gel science: The physics and chemistry of sol-gel processing*, Academic Press. Inc., London 1990, chapter 2.

[78] J. Y. Kim, S. H. Kim, H. H. Lee, K. Lee, W. Ma, X. Gong, A. J. Heeger, *Adv. Mater.* **2006**, *18*, 572.

[79] S. H. Park, A. Roy, S. Beaupre', S. N. Cho, N. Coates, J. S. Moon, D. Moses, M. Leclerc, K. H. Lee, A. J. Heeger, *Nat. Photonics* **2009**, *3*, 297.

[80] A. Hayakawa, O. Yoshikawa, T. Fujieda, K. Uehara, S. Yoshikawa, *Appl. Phys. Lett.* **2007**, *90*, 163517.

[81] Z. Tan, C. Yang, E. Zhou, X. Wang, Y. Li, *Appl. Phys. Lett.* **2007**, *91*, 023509.

[82] S. J. Yoon, J. H. Park, H. K. Lee, O. O. Park, *Appl. Phys. Lett.* **2008**, *92*, 143504.

[83] P. Schilinsky, C. Waldauf, C. J. Brabec, *Appl. Phys. Lett.* **2002**, *81*, 3885.

[84] R. Pacios, A. J. Chatten, K. Kawano, J. R. Durrant, D. D. C. Bradley, J. Nelson, *Adv. Funct. Mater.* **2006**, *16*, 2117.

[85] D. H. Wang, D. G. Choi, K. J. Lee, O. O. Park, J. H. Park, *Org. Electron.* **2010**, *11*, 599.

[86] W. J. H. Van Gennip, J. K. J. Van Duren, P. C. Thüne, R. A. J. Janssen, J. W. Niemantsverdriet, *J. Chem. Phys.* **2002**, *117*, 5031.

[87] J.-N. Audinot, P. Lévêque, R. Bechara, N. Leclerc, J. Guillot, H.-N. Migeon, G. Hadziioannou, T. Heiser, *Surf. Interface Anal.* **2010**, DOI 10.1002/sia.3359.

[88] A. C. Dürr, F. Schreiber, M. Kelsch, H. D. Carstanjen, H. Dosch, *Adv. Mater.* **2002**, *14*, 961.

[89] C. M. Ramsdale, J. A. Barker, A. C. Arias, J. D. MacKenzie, R. H. Friend, N. C. Greenham, *J. Appl. Phys.* **2002**, *92*, 4266.

[90] C. J. Brabec, A. Cravino, D. Meissner, N. S. Sariciftci, T. Fromherz, M. T. Rispens, L. Sanchez, J. C. Hummelen, *Adv. Funct. Mater.* **2001**, *11*, 374.

[91] V. D. Mihailetchi, P. W. M. Blom, J. C. Hummelen, M. T. Rispens, *J. Appl. Phys.* **2003**, *94*, 6849.

[92] E. Ahlswede, J. Hanisch, M. Powall, *Appl. Phys. Lett.* **2007**, *90*, 163504.

[93] X. Jiang, H. Xu, L. Yang, M. Shi, M. Wang, H. Chen, *Sol. Energy Mater. Sol. Cells* **2009**, *93*, 650.

[94] F. Zhang, M. Ceder, O. Inganas, *Adv. Mater.* **2007**, *19*, 1835.

[95] S.-H. Oh, S.-I. Na, J. Jo, B. Lim, D. Vak, D.-Y. Kim, *Adv. Funct. Mater.* **2010**, *20*, 1977.

[96] C. M. Ramsdale, J. A. Barker, A. C. Arias, J. D. MacKenzie, R. H. Friend, N. C. Greenham, *J. Appl. Phys.* **2002**, *92*, 4266.

[97] V. D. Mihailetchi, P. W. M. Blom, J. C. Hummelen, M. T. Rispens, *J. Appl. Phys.* **2003**, *94*, 6849.

[98] P. Peumans, V. Bulovic, S. R. Forrest, *Appl. Phys. Lett.* **2000**, *76*, 2650.

[99] H. Gommans, B. Verreet, B. P. Rand, R. Muller, J. Poortmans, P. Heremans, J. Genoe, *Adv. Funct. Mater.* **2008**, *18*, 3686.

[100] S. O. Jeon, K. S. Yook, C. W. Joo, J. Y. Lee, *J. Mater. Chem.* **2009**, *19*, 5940.

[101] S. O. Jeon, K. S. Yook, B. D. Chin, Y. S. Park, J. Y. Lee, *Sol. Energy Mater. Sol. Cells* **2010**, in press.

[102] D. H. Wang, D. G. Choi, K. J. Lee, J. H. Jeong, S. H. Jeon, O. O. Park, J. H. Park, *Org. Electron.* **2010**, *11*, 285.

[103] J. H. Lee, D. W. Kim, H. Jang, J. K. Choi, J. Geng, J. W. Jung, S. C. Yoon, H. T. Jung, *Small* **2009**, *5*, 2139.

[104] S. I. Na, S. S. Kim, J. Jo, S. H. Oh, J. Kim, D. Y. Kim, *Adv. Funct. Mater.* **2008**, *18*, 3956.

[105] H. K. Lee, J. H. Jeon, D. H. Wang, O. O. Park, J. K. Kim, S. H. Im, J. H. Park, *Appl. Phys. Lett.* **2010**, *96*, 103304.